machines

MDPI

Article

Improved FMEA Risk Assessment Based on Load Sharing and Its Application to a Magnetic Lifting System

Bo Sun *, Lei Wang, Jian Zhang and Ning Ding

College of Mechanical and Vehicle Engineering, Changchun University, 6543 Satellite Road, Changchun 130022, China; 230101019@mails.ccu.edu.cn (L.W.); 240101002@mails.ccu.edu.cn (J.Z.); dingn@ccu.edu.cn (N.D.)
* Correspondence: sunb@ccu.edu.cn

Abstract

Failure Mode and Effects Analysis (FMEA) is a systematic risk assessment tool that effectively evaluates the safety and reliability of products prior to their deployment. However, traditional FMEA fails to consider and leverage inherent system-specific information during risk assessment, while also neglecting the weights of risk factors (RFs) when processing data related to the Risk Priority Number (RPN). This leads to significant subjectivity in the final risk ranking of failure modes. To overcome these drawbacks, this study proposes an improved FMEA risk assessment method based on load sharing, aiming to develop an improved FMEA method that addresses the critical limitations of traditional approaches by integrating load sharing principles and systematic weight determination, thereby enhancing risk assessment objectivity and accuracy in complex multi-component systems. First, probabilistic linguistic terms are adopted to quantify experts' risk assessment information, and the geometric mean method is then used to aggregate assessments from multiple experts. Second, the Fuzzy Best–Worst Method (FBWM) is employed to determine the relative weights of the three RPN factors (Occurrence, Severity, and Detection). Additionally, partial system structural data are obtained through load sharing, and these data—combined with the calculated factor weights—are integrated into the Technique for Order Preference by Similarity to Ideal Solution (TOPSIS) to generate the final risk ranking of failure modes. Finally, a case study of a magnetic crane is conducted to verify the feasibility and effectiveness of the proposed method, supplemented by comparative experiments to demonstrate its superiority.

Keywords: FMEA; RFs; load sharing; FBWM; TOPSIS

check for updates

Academic Editor: Alexios Papacharalampopoulos

Received: 29 October 2025
Revised: 20 November 2025
Accepted: 28 November 2025
Published: 2 December 2025

Citation: Sun, B.; Wang, L.; Zhang, J.; Ding, N. Improved FMEA Risk Assessment Based on Load Sharing and Its Application to a Magnetic Lifting System. *Machines* **2025**, *13*, 1113. https://doi.org/10.3390/machines13121113

Copyright: © 2025 by the authors. Licensee MDPI, Basel, Switzerland. This article is an open access article distributed under the terms and conditions of the Creative Commons Attribution (CC BY) license (https://creativecommons.org/licenses/by/4.0/).

1. Introduction

Failure Mode and Effects Analysis (FMEA) [1,2] is a systematic analysis method widely used in the field of reliability engineering. The calculation process of traditional FMEA consists of three steps. First, experts conduct risk rating on the Severity (S), Occurrence (O), and Detection (D) among the risk factors (RFs) of product failure modes to obtain the RF values for all failure modes. Second, the S, O, and D values of each failure mode are multiplied respectively to obtain the Risk Priority Number (RPN) for that failure mode. Finally, ranking is performed based on the RPN values of each failure mode, resulting in the risk ranking of failure modes. This method conducts quantitative ranking of various risks. By prioritizing the handling of high-risk failure items and guiding teams to develop targeted preventive measures, it effectively avoids the occurrence of failures and enhances the reliability of systems and products. However, traditional FMEA [3] is highly

subjective and has several limitations [4] in practical applications: (1) simple rating fails to convey experts' subjective information; (2) it treats the weights of RFs as equal; (3) the RPN calculation is simplistic, leading to unreliable rankings; (4) the entire process fails to consider certain inherent information of the system itself.

Traditional FMEA typically uses numerical values from one to nine to represent risk levels, where a higher value indicates greater risk. However, such a simplistic rating system fails to capture experts' nuanced judgments. To address this issue, many scholars have introduced the concept of fuzziness. For instance, Tian et al. [5] proposed an interval number-based FMEA method for the risk assessment of electric vehicle charging piles, which effectively addressed the fuzziness of expert judgments by quantifying risk values into intervals. Their results indicated that the method could accurately identify high-risk failure modes such as charging interface overheating. Another example is Li [6], who successfully quantified the fuzziness and reliability of expert evaluations by integrating Z-numbers, accurately identifying high-risk failure modes in crane operations (e.g., hydraulic system leakage and brake system wear). Both approaches struggle to represent situations where experts simultaneously assign probabilities to multiple linguistic terms. While this limitation can lead to a notable information loss, Pang et al. [7] demonstrated that Probabilistic Linguistic Term Sets are specifically designed to preserve this information in FMEA contexts.

To resolve this, some scholars have introduced Linguistic Term Sets (LTSs) [8], such as Probabilistic Linguistic Term Sets (PLTSs) [9], Double Hierarchy Linguistic Term Sets [10], and Probabilistic Hesitant Fuzzy Linguistic Term Sets [11]. All of these approaches integrate LTSs with probability theory. Specifically, LTSs can accurately depict the risk levels in FMEA, while probability effectively quantifies the credibility of experts' judgments on these levels. Compared with interval-number-based methods, this LTS–probability combination conveys richer evaluation information. In contrast to Z-numbers, it is not only simpler, more intuitive, and easier to compute but also more user-friendly for experts, thereby reducing the evaluation threshold. In the FMEA calculation process, the weights of S, O, and D are usually treated as equal, which is irrational. As a result, numerous studies have focused on calculating the weights of S, O, and D in FMEA. For example, some methods rely on experts to directly assign weights, but this approach may lead to significant discrepancies in expert opinions. To mitigate this, scholars have introduced Multi-Criteria Decision Making (MCDM) [12] to calculate these weights. Kumari et al. [13] and Li et al. [14], for instance, proposed FMEA methods based on the Analytic Hierarchy Process (AHP), which computes weights by constructing a comparison matrix. Other examples are Rezaei et al. [15] and Pamučar et al. [16], who used the Best–Worst Method (BWM). They first identified the best and worst criteria to generate comparison data, and then calculated weights by solving a system of inequalities. Both BWM and AHP can reduce the subjectivity of risk assessment results. Compared with AHP, BWM requires fewer pairwise comparisons, thus reducing subjectivity more effectively. This study will adopt a method that combines LTS–probability integration with BWM to achieve the quantification of risk assessment and the calculation of RF weights.

With the development of combinations of FMEA and MCDM [17–19], methods that integrate multiple MCDMs have emerged. In FMEA-MCDM combinations, experts typically provide data in two tables: one contains data on the mutual comparisons of S, O, and D, and the other includes data on S, O, and D for each failure mode of the system. Typically, subjective weighting methods such as AHP and BWM are used to calculate subjective weights based on the former set of data. Then, objective weighting methods like the entropy weight method and Criteria Importance Through Inter-criteria Correlation (CRITIC) [20] are applied to compute objective weights using the latter set of data.

Finally, parameters are used to adjust the proportion of subjective and objective weights, resulting in the final comprehensive weights. For example, Wang et al. [11] developed and successfully applied an integrated weighting methodology combining the Best–Worst Method (BWM) and Multi-Dimensional Decision Making (MDM) to determine the weights of risk factors (RFs) for machine tools. Their research demonstrated that this comprehensive weighting approach not only effectively reduced the sensitivity of risk prioritization outcomes but also significantly mitigated the influence of subjective judgments on the evaluation process. However, both single weighting methods and comprehensive weight algorithms are based on experts' subjective evaluations and lack support from real-world conditions. This highlights a more fundamental limitation: the risk assessment process remains decoupled from the physical architecture of the system. Expert judgments, though valuable, cannot precisely quantify the physical dependencies between components and the effects of failure propagation. This disconnect can lead to risk prioritization that deviates from the true reliability profile of the system. Therefore, we propose an FMEA method based on load sharing, which obtains certain structural data by analyzing the structure of the research object to reduce the subjectivity of FMEA.

Load sharing [21,22] refers to the phenomenon in multi-component systems where components may interact with each other in different proportions during operation. When a component fails, its load is borne by adjacent components, which increases the likelihood of failure for those adjacent components. Specifically, the greater the load, the higher the probability of failure. In systems with both series and parallel connections, the severity of series connections is far greater than that of parallel connections. For series-connected components, the failure of any single component will lead to the failure of the entire system. In contrast, for parallel-connected components, the failure of one parallel component will result in the load being shared by other parallel components, and will not cause the entire system to fail. Therefore, this study is theoretically motivated by the integration of the load sharing model into the FMEA framework. The core rationale is to incorporate objective system structural information into risk assessment, creating a subjective–objective fusion. This allows for the quantification of failure propagation and system-level impact, shifting the focus from the "likelihood of component failure" to the "conditional probability of component failure causing system failure." A component with a high O value might pose a low actual risk if it is surrounded by sufficient redundancy (parallel structure), whereas a component with a moderate O value but located in a critical serial path might have its risk severely underestimated. This approach fundamentally differs from existing MCDM-FMEA methods by introducing inherent, objective information dictated by the physical system structure, ensuring the final risk ranking reflects not only what the risk experts "perceive" but also what the risk the system structure "reveals".

In FMEA risk ranking, the product calculation of O, S, and D is overly simplistic. Therefore, many scholars have introduced MCDM-based ranking methods. VlseKriterijumska Optimizacija I Kompromisno Resenje (VIKOR) [23] and Technique for Order Preference by Similarity to Ideal Solution (TOPSIS) [24,25] are two commonly used MCDM methods. The VIKOR method performs well in handling conflicting objectives, while the TOPSIS method focuses more on the proximity of alternatives to the ideal solution. These ranking methods are usually used in combination with approaches such as BWM, AHP, and comprehensive weighting methods. Typically, relative weights are first calculated via MCDM and then integrated into VIKOR or TOPSIS for ranking. This study will simultaneously integrate the data obtained from load sharing and the original data into TOPSIS to generate the final risk ranking.

The structure of this study is as follows: Section 2 presents the preliminaries of load sharing. Sections 3.1 and 3.2 introduce the FBWM method combining LTS with probability,

which is used for the quantification of experts' risk assessments and the calculation of RF weights. Section 3.3 focuses on load sharing: by analyzing the spatial states of failure modes, the probability of each failure mode causing system failure is derived based on the O values provided by experts. Section 3.4 covers TOPSIS-based ranking: the values obtained from load sharing and the original S, O, and D values are simultaneously integrated into TOPSIS to obtain the final risk ranking. Section 4 presents a case study applying the proposed method to a magnetic lifting system, supplemented by sensitivity and comparative analyses. The paper concludes with research findings and future directions in Section 5.

2. Load Sharing Method

A load sharing system [26] is a redundant architecture composed of functionally parallel and interdependent components. Under normal operating conditions, all components in the system collectively bear the operational load. Its core characteristic is that, when one or more components fail, the system does not immediately cease to function; instead, it dynamically redistributes the load previously borne by the failed components to the remaining operational ones.

We consider the spatial arrangement relationship of each component, where θ_{ij} represents the connection relationship between the non-faulty component i and the faulty component j. $\theta_{ij} = 1$ indicates a connection exists and $\theta_{ij} = 0$ indicates no connection. Here, $i = 1, 2, \ldots, n; j = 1, 2, \ldots, n$, with n being the total number of components.

$$\begin{pmatrix} \theta_{11} & \theta_{12} & \cdots & \theta_{1n} \\ \theta_{21} & \theta_{22} & \cdots & \theta_{2n} \\ \vdots & \vdots & \ddots & \vdots \\ \theta_{n1} & \theta_{n2} & \vdots & \theta_{nn} \end{pmatrix} \tag{1}$$

To distribute the load of a faulty component proportionally among each non-faulty component, a normalization process is performed on each column, as shown in Formula (2). Finally, we obtain a matrix V, where v_{ij} represents the load proportion of each faulty component relative to the surrounding components.

$$v_{ij} = \frac{\theta_{ij}}{\sum_{i=1}^{n} \theta_{ij}} \tag{2}$$

$$V = \begin{pmatrix} v_{11} & v_{12} & \cdots & v_{1n} \\ v_{21} & v_{22} & \cdots & v_{2n} \\ \vdots & \vdots & \ddots & \vdots \\ v_{n1} & v_{n2} & \vdots & v_{nn} \end{pmatrix} \tag{3}$$

The number of spatial neighbors of a component is determined by the number of its connections to other components. The total load L of the system is shared by all components, which are allocated the total load L in the proportion of $r_1, r_2, \ldots r_n$. The system fails when the total load borne by the non-faulty components is less than the total load L. z_i denotes the initial load of the i-th component.

$$z_i = \frac{r_i L}{\sum_{i=1}^{n} r_i} \tag{4}$$

Define $z_{i(j)}$ as the load of component i when the faulty component j fails; the formula is shown in Formula (5).

$$z_{i(j)} = z_i + v_{ij} z_j \tag{5}$$

If component k, which is adjacent to component i, also fails when the faulty component j is in a failed state, the situation is as shown in Formula (6).

$$z_{i(j,k)} = z_{i(j)} + v_{ik}z_k = z_i + v_{ij}z_j + v_{ik}z_k \quad (6)$$

The system fails when the total load of the working components is less than the total load applied to the system, i.e., $\sum_{i=1}^{n} z_i < L$.

To explain under what circumstances the system fails, let us consider a four-component parallel gear system, as shown in Figure 1. Component systems A and B are connected by a shaft, while component systems C and D are connected by another shaft. When component system A fails, its load is entirely transferred to component system B; systems C and D remain unaffected. However, if gear system B also fails after the failure of gear system A, the combined load of both A and B cannot be transferred to any other component, causing the entire system to halt.

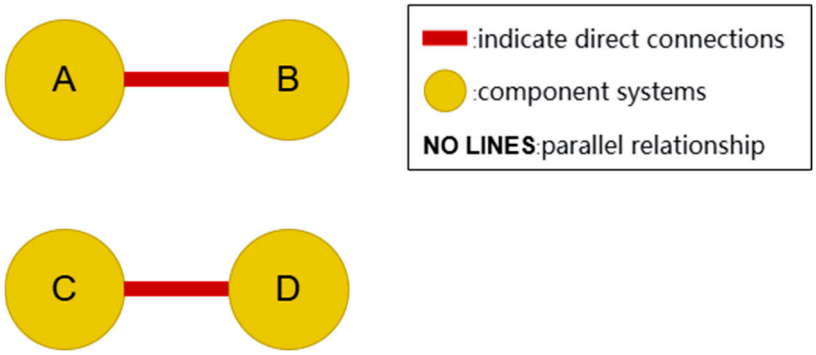


Figure 1. Four-component system.

In summary, the core value of the load sharing model lies in its ability to translate the physical topology of a system—the connectivity between components into dynamic, quantifiable reliability parameters. By simulating failure propagation paths and load redistribution processes, it reveals how local failures can evolve into system-level failures through intrinsic systemic interdependencies. This model provides the theoretical basis and a computational framework for assessing the system-level impact of component failures. Thereby, it incorporates the often-overlooked characteristics of system architecture into traditional reliability analysis, laying a solid foundation for its subsequent integration with the FMEA methodology to conduct more comprehensive risk assessments.

3. Methodology

The method proposed in this paper is mainly divided into four parts. The first part is the PLTS method constructed by LTS and probability, which is used to quantify expert evaluation information. The second part is FBWM, which is applied to calculate the weights of RFs. The third part is load sharing, which deduces the probability of system failure caused by the occurrence of all fault modes based on the evaluation information of O. The fourth part is TOPSIS, which integrates the derived data into the original data for risk ranking, as specifically shown in Figure 2.

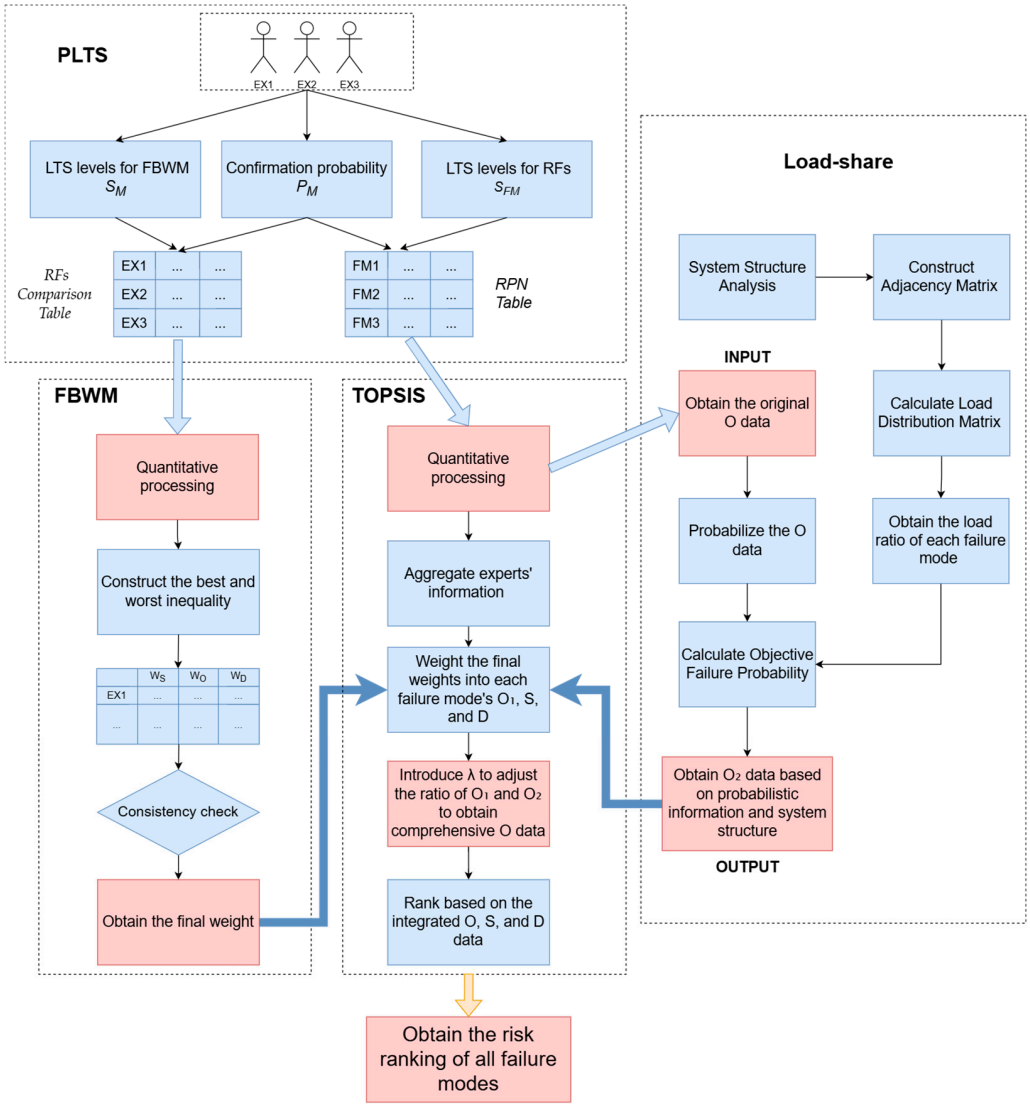


Figure 2. Methodology flow chart.

3.1. PLTS

In this section, we will define risk assessment criteria using the LTS and construct a PLTS risk assessment framework combined with probability, which is used for the collection and calculation of expert evaluation information.

Step 1: Define Risk Assessment Criteria

In the PLTS framework, two risk assessment criteria need to be defined. One is the standard S_{FM} for all fault mode RFs provided during the risk assessment phase, and the other is the comparison standard S_M for RFs provided when calculating the weights of RFs.

$$S_{\mathrm{FM}} = \begin{cases} s_1 = Absolutely\ \mathrm{Low}(AL) \\ \mathrm{s}_2 = Very\ \mathrm{Low}(VL) \\ s_3 = Low(L) \\ s_4 = \mathrm{Moderate\ Low}(ML) \\ s_5 = Moderate(M) \\ s_6 = \mathrm{Moderate\ High}(MH) \\ s_7 = High(H) \\ s_8 = Very\ \mathrm{High}(VH) \\ s_9 = Absolutely\ \mathrm{High}(AH) \end{cases} \tag{7}$$

$$S_M = \begin{cases} m_1 = Equal\ important(EI) \\ m_2 = Very\ weak\ important(VWI) \\ m_3 = Weak\ important(WI) \\ m_4 = Very\ \text{moderate}\ important(VMI) \\ m_5 = Moderate\ \text{important}(MI) \\ m_6 = Strong\ \text{important}(SI) \\ m_7 = Very\ \text{strong important}(VSI) \\ m_8 = Very\ \text{important}(VI) \\ m_9 = Extreme\ \text{important}(EI) \end{cases} \tag{8}$$

Step 2: Define the Confirmation Probability Criterion

Specify the confirmation probability P_M, which is used to verify the reliability of Criteria (7) and (8) during the experts' risk assessment process.

$$P_M = \begin{cases} p_1 = Absolutely\ Reliable(AR)(0.9) \\ p_2 = Very\ Highly\ Reliable(VHR)(0.8) \\ p_3 = Highly\ Reliable(HR)(0.7) \\ \mathrm{p}_4 = Equally\ \text{Reliable}(ER)(0.5) \\ p_5 = Weakly\ Reliable(WR)(0.3) \\ p_6 = Very\ Weakly\ Reliable(VWR)(0.2) \\ p_7 = Absolutely\ Unreliable(AU)(0.1) \end{cases} \tag{9}$$

Step 3: Standard Form of Expert Evaluation

We ask experts to select criteria from (7) to conduct risk assessment on the RFs of fault modes and provide the corresponding confirmation probability for Criterion (9). If an expert only adopts one criterion for the RFs of a fault mode, i.e., the set $S = \{s_i\}$, it can be denoted as $\{(s_i, p_j)\}$. If the expert hesitates about the k-th criterion, it can be denoted as $\{(s_i, p_j), (s_k, 1 - p_j)\}$. Therefore, the representation form of the fault mode is as shown in Formula (10).

$$DM = \left\{ \begin{array}{ll} \{(s_i, p_j) | i = 1, 2, \ldots, 9; j = 1, 2, \ldots, 6\} & \\ \{(s_i, p_j), (s_k, 1 - p_j) | k = 1, 2 \ldots 9\} & if\ \exists\ s_k \in S \end{array} \right\} \tag{10}$$

For example, if an expert evaluates the RFs of a certain fault mode DM_1 as s_7 and provides a confirmation probability of p_1 for s_7, but hesitates about the criterion s_8, the expert's evaluation can be denoted as $DM_1 = \{(s_7, p_1), (s_8, 1 - p_1)\}$.

Step 4: Quantify Risk Assessment Information

If the risk assessment information is denoted in the form of Formula (10), the score is obtained by multiplying each LTS level by its corresponding probability and then summing the products. As shown in Formula (11), score formulae for the two scenarios are derived.

$$D_{DM} = \left\{ \begin{array}{ll} i \times p_j & \\ i \times p_j + k \times (1 - p_j) & if\ \exists\ s_k \in S \end{array} \right\} \tag{11}$$

Step 5: Aggregate Experts' Risk Assessment Data

If m experts provide evaluation results as $\{D_{DM1}, D_{DM2}, \ldots, D_{DMm}\}$, the aggregation formula [27] is as shown in Formula (12).

$$D = (D_{DM1} \times D_{DM2} \times \cdots \times D_{DMm})^{\frac{1}{\mathrm{m}}} \tag{12}$$

The PLTS framework effectively quantifies expert judgments in FMEA by combining linguistic terms with probability distributions. It preserves critical assessment information

while minimizing information loss, serving as a vital input for subsequent FBWM and load sharing analyses in our integrated risk evaluation methodology.

3.2. FBWM

The BWM is a new weight calculation method proposed by Rezaei (2015) [15]. This section will describe the process of calculating weights using the Fuzzy Best–Worst Method (FBWM).

Step 1: Confirm the Decision Criteria

In this step, we will determine which criteria to calculate weights for. Assume there are n decision criteria, and these criteria form the set $A = \{a_1, a_2, \ldots, a_n\}$.

Step 2: Identify the Best and Worst Criteria Among All Criteria

In this step, experts are required to select the best criterion a_B and the worst criterion a_W from set A based on the decision criteria.

Step 3: Construct Comparison Relationships

Construct two sets of comparison data, a_B and a_W, which are derived from comparing A_B and A_W with each criterion the set A, respectively.

$$\left\{ \begin{array}{c} A_B = (a_{B1}, a_{B2}, \ldots, a_{Bn}) \\ A_W = (a_{1W}, a_{2W}, \ldots, a_{nW})^T \end{array} \right\} \tag{13}$$

a_{B1} represents the multiple of the best criterion a_B relative to criterion a_1, and a_{1W} represents the multiple of criterion a_1 relative to the worst criterion a_W. Here, both a_{BB} and a_{WW} are equal to 1.

Step 4: Determine the Optimal Weights

In this step, we assume the final weights of the criteria are $w = (w_1, w_2, \ldots, w_n)$, where the weights corresponding to a_B and a_W are w_B and w_W, respectively. In the comparison data, a_{B1} is the value of a_B/a_1, and this value should be close to w_B/w_1. Therefore, we transform the problem into finding w, such that the maximum values of $\left|w_B/w_j - a_{Bj}\right|$ and $\left|w_j/w_W - a_{jW}\right|$ are both less than a very small number ξ^*, as shown in Formula (14).

$$\left\{ \begin{array}{l} \left|\frac{w_B}{w_j} - a_{Bj}\right| \le \xi^*, \forall \, j \\ \left|\frac{w_B}{w_j} - a_{Bj}\right| \le \xi^*, \forall \, j \\ \sum_{j=1}^{n} w_j = 1 \\ w_j \ge 0 \end{array} \right. \tag{14}$$

Step 5: Consistency Check

The FBWM is based on comparison data, so a consistency check is required. The consistency check formula for BWM is shown in Formula (15) [28].

$$CR = \frac{\xi^*}{\xi} \tag{15}$$

Here, ξ is determined by a_{BW}. However, in a fuzzy environment, the value of a_{BW} is a fraction, so it is calculated using Formula (16) [28].

$$(a_{BW} - \xi) \times (a_{BW} - \xi) = a_{BW} + \xi \tag{16}$$

Typically, there are two solutions for ξ, and the smaller one is selected as the criterion. If $CR \le 0.1$, the consistency check is passed.

This section has established the FBWM as a robust approach for determining risk factor weights in FMEA. By incorporating PLTS to address uncertainties in expert judg-

ment, FBWM preserves the efficiency of traditional BWM while significantly enhancing its capacity to capture subjective ambiguity.

3.3. FMEA and Load Sharing

In FMEA, experts provide numerical values for the O, S, and D of failure modes to rank the failures. Typically, the weights of O, S, and D are calculated by combining them with MCDM methods, which are then integrated into the RPN table for ranking. However, both the data from MCDM and the data in the RPN table are based on experts' subjective evaluations. Therefore, we analyze the occurrence probability (O) through experts' opinions and, in combination with the system structure, calculate under what circumstances the failure of each component will lead to the failure of the entire system.

Step 1: Obtain the Failure Probability of Components

Experts provide the O values for each of the n failure modes in FMEA, denoted as $O = \{o_1, o_2, \ldots, o_n\}$. Using the evaluation criteria S_{FM} presented in Section 3.1, O is processed via Formula (17) to convert it into a probability format, where $MAX(S_{FM})$ represents the highest index (set to 9 in this paper). This yields the occurrence probability of each mode as $E = \{e_1, e_2, \ldots, e_n\}$.

$$e_i = \frac{o_i}{MAX(S_{FM})} \tag{17}$$

Step 2: Define the Failure Probability of the Next State

Assume that, when component $j_1, j_2, \ldots, j_n$ around component i fails, the load on component i will increase, and thus its probability of failure will rise, as expressed in Formula (18).

$$e_{i(j_1,j_2,\ldots j_n)} = (1 + \frac{z_{i(j_1,j_2,\ldots j_n)}}{L})e_i \tag{18}$$

Step 3: Probability of Component Failure

A component's failure will lead to the failure of the entire system only when all adjacent components that can share its load have failed. Therefore, the probability of a component failure causing the entire system to fail is taken as the probability of that failure mode.

If there are n components around component i, the probability of component i failing when all surrounding components have failed is shown in Formula (18), where i is the target component and $j_1, j_2, \ldots, j_n$ represent the independent failure sequences of the surrounding components.

By multiplying the probabilities s of all states prior to the system failure, the final probability $F_{i(j_1,j_2,j_3,\ldots,j_n)}$ is obtained, as shown in Formula (19).

$$F_{i(j_1,j_2,j_3,\ldots,j_n)} = e_{j_1} \times e_{j_2(j_1)} \times e_{j_3(j_1,j_2)} \times \cdots \times e_{j_n(j_1,j_2,\ldots,j_{n-1})} \times e_{i(j_1,j_2,\ldots j_n)} \tag{19}$$

When there are correlations between $j_1, j_2, \ldots, j_m$, different failure sequences may lead to different final outcomes. Therefore, we propose a weighting calculation method to aggregate the results from different sequences, as shown in Formula (20).

$$F_i = w_1 \times F_{i(j_1,j_2,j_3,\ldots,j_m)} + w_2 \times F_{i(j_2,j_1,j_3,\ldots,j_m)} + \ldots, + w_{m!} \times F_{i(j_m,j_{m-1},j_{m-2},\ldots,j_1)} \tag{20}$$

Here, $w_1, w_2, \ldots, w_{m!}$ denote the respective weight coefficients assigned to each potential sequence.

This section integrated load sharing modeling with FMEA, enhancing risk assessment by quantifying how component failures propagate through system structures. This physics-

based approach complements expert judgment with objective data, improving failure mode prioritization accuracy.

The detailed derivation of the load sharing model and the calculation of weight are provided in Appendix A.

3.4. TOPSIS

TOPSIS is a well-established MCDM method [29]. Its core concept is based on the idea that the optimal alternative should have the shortest geometric distance from the positive ideal solution (PIS) and the longest geometric distance from the negative ideal solution (NIS). The PIS is a hypothetical solution that comprises the best values for all criteria, whereas the NIS consists of the worst values. TOPSIS is adopted in this study for the final risk ranking due to its intuitive logic, computational simplicity, and its ability to provide a comprehensive framework for simultaneously handling both the objective data derived from load sharing and the subjective data from expert evaluations.

Step 1: Process Subjective and Load Sharing Data

In load sharing, we obtained some structural data from FMEA. Since the data scale differs from that of S, O, and D, normalization [30] is performed in Formula (21) as follows:

$$b_i = \frac{a_i - \min(a_j)}{\max(a_j) - \min(a_j)}, i = 1, 2, \ldots, n; j = 1, 2, \ldots, n \tag{21}$$

where $(a_1, a_2, \ldots, a_n)$ denotes the data to be processed.

After standardizing all of the O-data F obtained from load sharing using Formula (21), we denote the processed data as $O_F^* = (O_1^*, O_2^*, \ldots, O_n^*)$, where n is the number of failed components.

There are m experts evaluate the S, O, and D of the failed components, yielding respective evaluations $S^i = (s_1^i, s_2^i, \ldots, s_n^i)$, $O^i = (o_1^i, o_2^i, \ldots, o_n^i)$, and $D^i = (d_1^i, d_2^i, \ldots, d_n^i)$. All experts' S, O, and D data are standardized via Formula (21) to obtain the aggregated values $S = (s_1, s_2, \ldots s_n)$, $O = (o_1^*, o_2^*, \ldots o_n^*)$, and $D = (d_1, d_2, \ldots d_n)$.

We then introduce the parameter λ to adjust the proportion between O (aggregated expert evaluation) and O_k^* (load sharing-derived data), as shown in Formula (22). This yields the comprehensive occurrence probability $T^* = (t_1^*.t_2^*, \ldots t_n^*)$.

$$t_i^* = (1 - \lambda)o_i^* + \lambda O_i^* \tag{22}$$

Here, λ denotes the ratio of the initial o_i to the structural O_i^*.

Step 2: Integrate BWM-Derived Weights into TOPSIS

Multiply the weights obtained via the FBWM by the matrix composed of S, O^*, and D, as shown in Formula (23).

$$M = \begin{pmatrix} s_1 \times w_1 & t_1^* \times w_2 & d_1 \times w_3 \\ s_2 \times w_1 & t_2^* \times w_2 & d_2 \times w_3 \\ \vdots & \vdots & \vdots \\ s_n \times w_1 & t_3^* \times w_2 & d_n \times w_3 \end{pmatrix} = \begin{pmatrix} t_{11} & t_{12} & t_{13} \\ t_{21} & t_{22} & t_{23} \\ \vdots & \vdots & \vdots \\ t_{n1} & t_{n2} & t_{n3} \end{pmatrix} \tag{23}$$

Step 3: Determine the Distance of Each Alternative to the Positive and Negative Ideal Solutions

A positive ideal solution and a negative ideal solution are identified for each column, as shown in Formula (24).

$$\begin{cases} A^+ = \begin{pmatrix} \max(t_{i1}) & \max(t_{i2}) & \max(t_{i3}) \end{pmatrix} \\ A^- = \begin{pmatrix} \min(t_{i1}) & \min(t_{i2}) & \min(t_{i3}) \end{pmatrix} \end{cases}, i = 1, 2, \ldots, n \tag{24}$$

Calculate the distance of each alternative to the positive ideal solution and the negative ideal solution.

$$\begin{cases} S_j^+ = \sqrt{[t_{j1} - \max(t_{i1})]^2 + [t_{j2} - \max(t_{i2})]^2 + [t_{j1} - \max(t_{i2})]^2} \\ S_j^- = \sqrt{[t_{j1} - \min(t_{i1})]^2 + [t_{j2} - \min(t_{i2})]^2 + [t_{j1} - \min(t_{i2})]^2} \\ j = 1, 2, \ldots, n \end{cases} \tag{25}$$

Step 4: Calculate the Relative Closeness of Each Alternative to the Ideal Solution

Finally, ranking is performed based on the C_i values with the calculation formula shown in Formula (26).

$$C_i = \frac{S_i^-}{S_i^- + S_i^+}, i = 1, 2, \ldots, n, C_i \in (0, 1) \tag{26}$$

In summary, the TOPSIS method enables the integration of the weighted S, O, and D values (obtained via FBWM) and the comprehensive occurrence probability O^* (which fuses expert assessments and load sharing data) into a unified decision matrix. By calculating the relative closeness C_i of each failure mode to the ideal solutions, a scientifically grounded and rational risk priority ranking is generated. This approach effectively mitigates the inherent limitations of the traditional RPN method, such as its simplistic calculation and strong subjectivity, leading to a more robust and reliable risk assessment outcome.

4. Application of Multi-Magnetic System

4.1. Case of Magnetic Crane

Compared with traditional electromagnetic hoists, a multi-magnetic system lifting permanent magnets for uneven surfaces has advantages, such as low energy consumption and a simple structure. However, safety issues [31,32] may arise during operation, making reliability analysis extremely necessary.

This type of permanent magnet, as shown in Figure 3, consists of a transmission mechanism, a magnetic system, and a movable pole face mechanism. The traditional transmission mechanism is composed of an internal gear mechanism (housed in a cover) and a chain hoist, which drives the rotation of composite permanent magnets in the magnetic system to achieve magnetic circuit switching. The magnetic system is made up of permanent magnets, conductors, and insulators, fulfilling the function of lifting heavy objects. The movable pole face mechanism comprises numerous movable magnetic poles, which can fit uneven surfaces to a greater extent and enhance the load-carrying capacity for workpieces with uneven surfaces. Based on its working principle, the FMEA is constructed, as shown in Table 1.

Three domain experts were invited to provide risk assessments in this case study. The selection criteria were rigorously defined to ensure the reliability and authority of the evaluations. All experts possess substantial professional experience (over 3 years) in relevant fields and are proficient in the FMEA methodology. Crucially, all experts were directly involved in the research and development of the specific multi-magnetic system lifting permanent magnets under investigation, guaranteeing that their assessments are grounded in profound system-specific knowledge. The detailed profiles of the experts are summarized in Table 2.

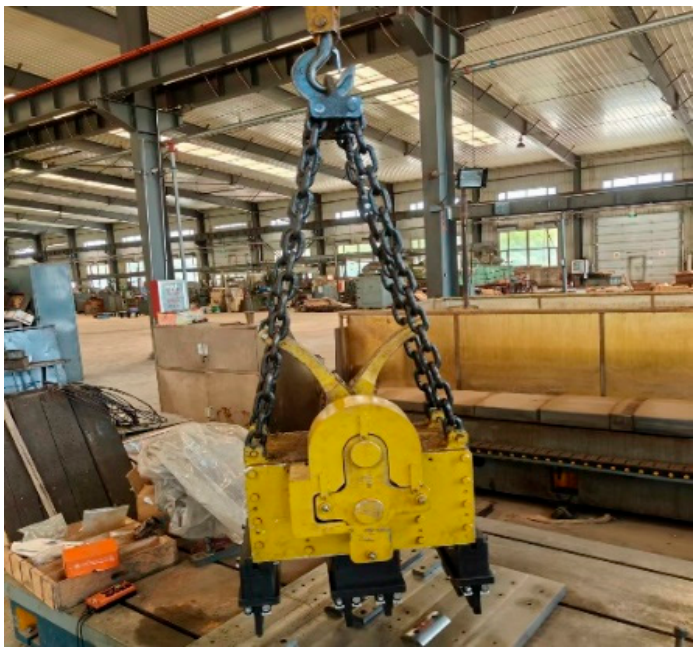


Figure 3. Actual scene diagram of the multi-magnetic system lifting permanent magnets for uneven surfaces.

Table 1. FMEA failure modes of the multi-magnetic system lifting permanent magnets for uneven surfaces.

Structure Group	Function	Item	Failed Component
Transmission Mechanism	Magnetic Circuit Switching	FM1	Ratcheting Chain Fracture
		FM2	Box Chain Fracture
		FM3	Ratchet Wear
		FM4	Gear Wear
		FM5	Rotating Shaft Wear
Magnetic System	Lifting Heavy Objects	FM6	Permanent Magnet Failure
		FM7	Outer Yoke Failure
		FM8	Inner Yoke Failure
		FM9	Pole Shoe Failure
Movable Pole Face Mechanism	Achieve a higher degree of fit with the workpiece surface	FM10	T-Type Movable Pole Jamming
		FM11	Stopper Movable Pole Jamming
		FM12	Cam Jamming

Table 2. Expert's information.

Expert	Experience	Years of Study
EX1	Responsible for the full-cycle development of the multi-magnetic system lifting permanent magnets, from design to manufacturing	10
EX2	The critical optimization of the movable pole face mechanism	3
EX3	Design phase of the movable pole face mechanism	3

When conducting FBWM weight calculation, experts first provide the best and worst data, as shown in Table 3. Then, the data are processed using Formula (11) to obtain quantized results, which are presented in Table 4.

Table 3. Experts' RFs risk assessment information.

	Best	S	O	D	S	O	D	Worst
EX1	S	$\{(m_1, p_1)\}$	$\{(m_2, 1-p_2), (m_3, p_2)\}$	$\{(m_6, p_4), (m_5, 1-p_4)\}$	$\{(m_6, p_4), (m_5, 1-p_4)\}$	$\{(m_2, p_2), (m_3, 1-p_2)\}$	$\{(m_1, p_1)\}$	D
EX2	S	$\{(m_1, p_1)\}$	$\{(m_2, p_4), (m_3, 1-p_4)\}$	$\{(m_5, p_3), (m_6, 1-p_3)\}$	$\{(m_5, p_3), (m_6, 1-p_3)\}$	$\{(m_2, p_2), (m_3, 1-p_2)\}$	$\{(m_1, p_1)\}$	D
EX3	S	$\{(m_1, p_1)\}$	$\{(m_1, 1-p_2), (m_2, p_2)\}$	$\{(m_3, p_4), (m_4, 1-p_4)\}$	$\{(m_3, p_4), (m_4, 1-p_4)\}$	$\{(m_1, p_4), (m_3, 1-p_4)\}$	$\{(m_1, p_1)\}$	D

Table 4. Quantized RF comparison data.

	Best	S	O	D	S	O	D	Worst
EX1	S	1	2.8	5.5	5.5	2.2	1	D
EX2	S	1	2.5	5.3	5.3	2.2	1	D
EX3	S	1	1.8	3.5	3.5	2	1	D

BWM weights are calculated based on the data provided in Table 4, yielding individual expert weights and comprehensive weights, as shown in Table 5. The weight of S is the highest, followed by O, and D is the lowest. The CR (Consistency Ratio) values of the three experts are 0.02666667, 0.00877578, and 0.01142857, respectively, which all less than 0.1, indicating that the consistency test is passed.

Table 5. Weights of RFs.

	w_S	w_O	w_D	CR
EX1	0.64798851	0.23706897	0.11494253	0.02666667
EX2	0.62875817	0.25359477	0.11764706	0.00877578
EX3	0.54251012	0.30364372	0.15384615	0.01142857
	0.607304011	0.264471973	0.128224016	

Three experts were invited to conduct a risk assessment on the multi-magnetic system lifting permanent magnets for uneven surfaces, and risk assessment values for each failure mode were obtained. The data are shown in Table 6.

Based on the RPN table provided by the experts, the O values provided in Table 6 are quantized using Formula (11). The geometric mean method is then adopted to aggregate the experts' risk assessment data, resulting in the final O value of (27).

$$O_s = \{5.116211, 4.021056, 4.156698, 4.824871, 4.389922, 3.762889, 3.774155, 5.536702, 5.511272, 8.071689, 7.2074, 6.299471\} \quad (27)$$

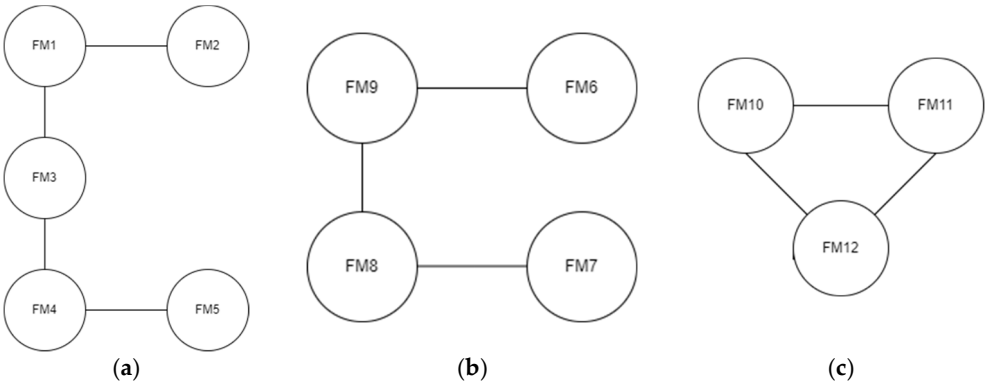
In Section 3.1, the highest evaluation index defined by experts is nine. The O_s is processed using Formula (17) to obtain the occurrence rate in probability form, denoted as O in Formula (28).

$$O = \{0.568468, 0.446784, 0.461855, 0.536097, 0.487769, 0.418099, 0.419351, 0.615189, 0.612364, 0.896854, 0.800822, 0.699941\} \quad (28)$$

Three spatial structure distributions are listed for the transmission mechanism, magnetic system, and movable pole face mechanism, as shown in Figure 4.

Table 6. RPN table of the multi-magnetic system lifting permanent magnets for uneven surfaces.

		S	O	D
FM1	EX1	$\{(s_4, p_2), (s_5, 1-p_2)\}$	$\{(s_6, p_2), (s_7, 1-p_2)\}$	$\{(s_2, p_2), (s_3, 1-p_2)\}$
	EX2	$\{(s_5, p_1)\}$	$\{(s_5, p_2), (s_4, 1-p_2)\}$	$\{(s_3, p_2)\}$
	EX3	$\{(s_5, p_3), (s_6, 1-p_3)\}$	$\{(s_5, p_1)\}$	$\{(s_2, p_4), (s_3, 1-p_4)\}$
FM2	EX1	$\{(s_9, p_3), (s_8, 1-p_3)\}$	$\{(s_4, p_3), (s_5, 1-p_3)\}$	$\{(s_2, p_4), (s_3, 1-p_4)\}$
	EX2	$\{(s_8, p_1)\}$	$\{(s_4, p_2), (s_5, 1-p_2)\}$	$\{(s_2, p_2), (s_3, 1-p_2)\}$
	EX3	$\{(s_9, p_2)\}$	$\{(s_4, p_1)\}$	$\{(s_3, p_3), (s_4, 1-p_3)\}$
FM3	EX1	$\{(s_4, p_2), (s_5, 1-p_2)\}$	$\{(s_4, p_4), (s_5, 1-p_4)\}$	$\{(s_3, p_4), (s_4, 1-p_4)\}$
	EX2	$\{(s_5, p_2), (s_6, 1-p_2)\}$	$\{(s_4, p_2), (s_5, 1-p_2)\}$	$\{(s_3, p_2)\}$
	EX3	$\{(s_5, p_2)\}$	$\{(s_4, p_2), (s_3, 1-p_2)\}$	$\{(s_5, p_2)\}$
FM4	EX1	$\{(s_4, p_2), (s_5, 1-p_2)\}$	$\{(s_5, p_2), (s_6, 1-p_2)\}$	$\{(s_3, p_4), (s_4, 1-p_4)\}$
	EX2	$\{(s_5, p_1)\}$	$\{(s_5, p_1)\}$	$\{(s_4, p_2)\}$
	EX3	$\{(s_4, p_3), (s_5, 1-p_3)\}$	$\{(s_6, p_2)\}$	$\{(s_3, p_4), (s_4, 1-p_4)\}$
FM5	EX1	$\{(s_5, p_2), (s_4, 1-p_2)\}$	$\{(s_5, p_3), (s_4, 1-p_3)\}$	$\{(s_3, p_4), (s_5, 1-p_4)\}$
	EX2	$\{(s_5, p_1)\}$	$\{(s_5, p_2)\}$	$\{(s_4, p_2), (s_3, 1-p_2)\}$
	EX3	$\{(s_3, p_2), (s_4, 1-p_2)\}$	$\{(s_5, p_1)\}$	$\{(s_4, p_2)\}$
FM6	EX1	$\{(s_7, p_2), (s_8, 1-p_2)\}$	$\{(s_4, p_3), (s_3, 1-p_3)\}$	$\{(s_3, p_2), (s_4, 1-p_2)\}$
	EX2	$\{(s_7, p_1)\}$	$\{(s_3, p_2), (s_4, 1-p_2)\}$	$\{(s_6, p_2), (s_5, 1-p_2)\}$
	EX3	$\{(s_8, p_2)\}$	$\{(s_5, p_1)\}$	$\{(s_4, p_2)\}$
FM7	EX1	$\{(s_3, p_4), (s_4, 1-p_4)\}$	$\{(s_4, p_2), (s_5, 1-p_2)\}$	$\{(s_4, p_2), (s_5, 1-p_2)\}$
	EX2	$\{(s_4, p_2), (s_3, 1-p_2)\}$	$\{(s_3, p_2), (s_4, 1-p_2)\}$	$\{(s_5, p_4), (s_6, 1-p_4)\}$
	EX3	$\{(s_6, p_2), (s_7, 1-p_2)\}$	$\{(s_5, p_2)\}$	$\{(s_3, p_2), (s_2, 1-p_2)\}$
FM8	EX1	$\{(s_3, p_4), (s_5, 1-p_4)\}$	$\{(s_5, p_2), (s_6, 1-p_2)\}$	$\{(s_5, p_2), (s_6, 1-p_2)\}$
	EX2	$\{(s_4, p_4), (s_5, 1-p_4)\}$	$\{(s_6, p_2)\}$	$\{(s_6, p_4), (s_5, 1-p_4)\}$
	EX3	$\{(s_4, p_2), (s_5, 1-p_2)\}$	$\{(s_7, p_2), (s_6, 1-p_2)\}$	$\{(s_6, p_2)\}$
FM9	EX1	$\{(s_3, p_2), (s_4, 1-p_2)\}$	$\{(s_5, p_4), (s_7, 1-p_4)\}$	$\{(s_6, p_2), (s_5, 1-p_2)\}$
	EX2	$\{(s_2, p_2), (s_1, 1-p_2)\}$	$\{(s_6, p_2), (s_7, 1-p_2)\}$	$\{(s_5, p_2)\}$
	EX3	$\{(s_3, p_2)\}$	$\{(s_5, p_1)\}$	$\{(s_7, p_2)\}$
FM10	EX1	$\{(s_2, p_4), (s_3, 1-p_4)\}$	$\{(s_8, p_3), (s_9, 1-p_3)\}$	$\{(s_2, p_2), (s_3, 1-p_2)\}$
	EX2	$\{(s_2, p_2), (s_3, 1-p_2)\}$	$\{(s_9, p_2)\}$	$\{(s_2, p_2), (s_1, 1-p_2)\}$
	EX3	$\{(s_2, p_1)\}$	$\{(s_9, p_2), (s_8, 1-p_2)\}$	$\{(s_4, p_3), (s_3, 1-p_3)\}$
FM11	EX1	$\{(s_2, p_2), (s_3, 1-p_2)\}$	$\{(s_7, p_4), (s_8, 1-p_4)\}$	$\{(s_2, p_4), (s_3, 1-p_4)\}$
	EX2	$\{(s_3, p_1)\}$	$\{(s_8, p_2), (s_7, 1-p_2)\}$	$\{(s_3, p_2)\}$
	EX3	$\{(s_2, p_1)\}$	$\{(s_8, p_2)\}$	$\{(s_3, p_2), (s_2, 1-p_2)\}$
FM12	EX1	$\{(s_2, p_2), (s_3, 1-p_2)\}$	$\{(s_6, p_2), (s_7, 1-p_2)\}$	$\{(s_4, p_2), (s_5, 1-p_2)\}$
	EX2	$\{(s_2, p_4), (s_3, 1-p_4)\}$	$\{(s_7, p_2), (s_8, 1-p_2)\}$	$\{(s_6, p_2), (s_5, 1-p_2)\}$
	EX3	$\{(s_2, p_2), (s_3, 1-p_2)\}$	$\{(s_7, p_2)\}$	$\{(s_5, p_2)\}$



(**a**) (**b**) (**c**)

Figure 4. Spatial relationship of failure modes. (**a**) Transmission mechanism; (**b**) Magnetic system; (**c**) Movable pole face mechanism.

Among all failure modes, the failed components around FM1, FM2, FM3, FM4, FM5, FM6, FM7, FM8, and FM9 are mutually independent, so the impact of the failure sequence

of surrounding components on the results does not need to be considered. For FM10, FM11, and FM12, the failed components around them are interrelated, and the influence of the sequence must be taken into account. The final results obtained through calculation are shown in Formula (29).

$$O_F = \{0.141741, 0.28573, 0.164211, 0.145932, 0.294178, 0.288032, 0.290227, 0.190889, 0.19032, 0.65981, 0.65981, 0.65981\} \quad (29)$$

All RFs of the failure modes provided in Table 6 are quantized using Formula (11), and the geometric mean method is adopted to aggregate the risk assessment information from all experts, resulting in the values of S, O, and D. However, due to the different data scales between F and S, O, and D, the standardization process for S, O, D, and F is performed using Formula (21), and the final results are shown in Table 7.

Table 7. Standardized RPN table.

	$\mathbf{S^*}$	$\mathbf{O_F^*}$	$\mathbf{O^*}$	$\mathbf{D^*}$
FM1	0.453223	0.001	0.315083	0.001
FM2	1.001	0.278934	0.060916	0.095683
FM3	0.415722	0.044372	0.092396	0.309919
FM4	0.396597	0.009089	0.247468	0.370786
FM5	0.355375	0.29524	0.146524	0.46141
FM6	0.811309	0.283377	0.001	0.551302
FM7	0.400407	0.287615	0.003615	0.591554
FM8	0.377912	0.095868	0.412672	1.001
FM9	0.046779	0.094768	0.40677	0.967412
FM10	0.001	1.001	1.001	0.030928
FM11	0.011105	1.001	0.800413	0.071771
FM12	0.027902	1.001	0.589698	0.801735

Here, λ is introduced to integrate O^* and O_F^*, with the specific formula shown in Formula (22). In this method, a compromise approach is adopted ($\lambda = 0.5$) to synthesize O^* and O_F^*, and the comprehensive weights of S, O, and D from Table 6 are integrated into the aforementioned result. The final outcomes are presented in the following table.

The data in Table 8 are processed using TOPSIS. First, Formula (25) is used to calculate the distance to the positive ideal solution D^+ and the distance to the negative ideal solution D^- for each scheme. Then, Formula (26) is applied to obtain the relative C_i between each failure mode and the ideal solution. Finally, the risk ranking is determined based on the magnitude of C_i.

The final risk ranking, as presented in Table 9, provides a prioritized list for maintenance and design improvements. The high ranking of FM2 (Box Chain Fracture) and FM6 (Permanent Magnet Failure) as the top two critical failure modes is particularly noteworthy from an engineering perspective. FM2's top position is attributed to its high S score, indicating that its failure would have a catastrophic impact on the system's primary function of magnetic circuit switching. This aligns with engineering intuition, as a broken box chain would directly halt the lifting operation. Similarly, FM6 (Permanent Magnet Failure) ranks second due to its critical role in the magnetic system. A failure here would lead to a complete loss of lifting force, posing a severe safety hazard. The high ranking of these components underscores the need for robust design, high-quality materials, and preventative maintenance schedules specifically targeted at the chain assembly and permanent magnets to ensure operational safety and reliability.

Table 8. RPN table after FBWM processing.

	S	O	D
FM1	0.275244	0.041798	0.000128
FM2	0.607911	0.04494	0.012269
FM3	0.25247	0.018086	0.039739
FM4	0.240855	0.033926	0.047544
FM5	0.215821	0.058417	0.059164
FM6	0.492711	0.037605	0.07069
FM7	0.243169	0.038511	0.075851
FM8	0.229507	0.067247	0.128352
FM9	0.028409	0.066321	0.124045
FM10	0.000607	0.264736	0.003966
FM11	0.006744	0.238212	0.009203
FM12	0.016945	0.210348	0.102802

Table 9. Risk ranking of all failure modes.

	D^+	D^-	C_i	RANK
FM1	0.420488	0.275659	0.395978	3
FM2	0.248567	0.608019	0.709816	1
FM3	0.441619	0.254958	0.366015	6
FM4	0.44106	0.245394	0.35748	7
FM5	0.44843	0.226779	0.335865	8
FM6	0.261122	0.49752	0.655803	2
FM7	0.432402	0.254926	0.370895	5
FM8	0.426839	0.266934	0.384757	4
FM9	0.612544	0.13585	0.181522	12
FM10	0.619911	0.246681	0.284656	9
FM11	0.613435	0.220398	0.26432	11
FM12	0.594014	0.218571	0.268983	10

4.2. Sensitivity Analysis

To evaluate the robustness of the proposed method and understand the impact of key parameters on the risk ranking results, a comprehensive sensitivity analysis was conducted. The focus was on the parameter r, which governs the weighting between the expert-evaluated O^* and the load-sharing-derived O_F^*.

We adjust the value of λ and observe the changes in ranking under different proportions, with the results shown below (Figure 5).

As detailed in Table 10 and visualized in Figure 5, the failure mode rankings were calculated for a spectrum of λ values ranging from 0.1 to 0.9. The analysis reveals that the overall risk hierarchy is notably stable. Specifically, the top two failure modes (FM2 and FM6) and the bottom one (FM9) maintain their ranks across all scenarios. This stability in the extremities of the ranking list underscores the reliability of the proposed method in identifying the most critical and least critical failure modes, regardless of the chosen balance between subjective expert opinion and objective system structure data.

However, the analysis also provides valuable insights into how the system structure influences risk prioritization. The ranking of FM12 exhibits the most significant positive sensitivity to the parameter r. As r increases (giving more weight to the load sharing data O_F^*), FM12's rank consistently improves. This can be attributed to its two key characteristics: a high original expert-rated O value and few surrounding components in the spatial structure. In the load sharing model, a high O value combined with low redundancy (few components to share the load) results in a high O_F^* value, indicating a greater conditional

probability of causing system failure. Consequently, as the influence of O_F^* grows, FM12 is correctly identified as a more significant risk.

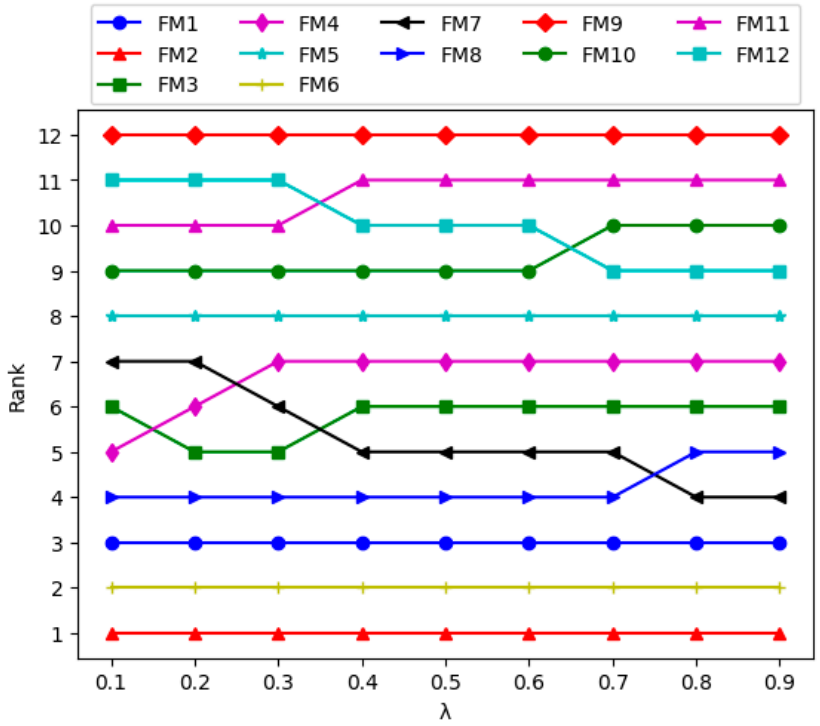


Figure 5. Visualization results of rankings under different λ values.

Table 10. Rankings under different λ values.

	λ	FM1	FM2	FM3	FM4	FM5	FM6	FM7	FM8	FM9	FM10	FM11	FM12
1	0.1	3	1	6	5	8	2	7	4	12	9	10	11
2	0.2	3	1	5	6	8	2	7	4	12	9	10	11
3	0.3	3	1	5	7	8	2	6	4	12	9	10	11
4	0.4	3	1	6	7	8	2	5	4	12	9	11	10
5	0.5	3	1	6	7	8	2	5	4	12	9	11	10
6	0.6	3	1	6	7	8	2	5	4	12	9	11	10
7	0.7	3	1	6	7	8	2	5	4	12	10	11	9
8	0.8	3	1	6	7	8	2	4	5	12	10	11	9
9	0.9	3	1	6	7	8	2	4	5	12	10	11	9

Conversely, failure modes like FM4, FM8, and FM9 show a slight downward trend in their rankings as r increases. These components are typically surrounded by a larger number of adjacent components. This higher degree of redundancy within the system architecture means that their failure is less likely to lead to a system-wide collapse, as the load can be effectively redistributed. Therefore, their load-sharing-derived O_F^* is relatively lower, and when these objective data are given more weight, their perceived risk decreases appropriately.

The sensitivity of FM7 and FM10 further validates the model's logical consistency. FM7, with fewer surrounding components, sees its rank increase with r, while FM10's position remains relatively stable but high due to its critical structural role.

In conclusion, the sensitivity analysis demonstrates that the proposed model is not overly sensitive to the specific choice of the parameter r. The core ranking is robust, while the observed fluctuations for specific failure modes are not random noise but are logically explained by and provide valuable insight into the underlying system reliability physics.

This enhances confidence in the method's practical utility for engineers, as it consistently highlights critical failures while providing a nuanced understanding of how system design influences risk.

4.3. Comparative Experiment

To validate the effectiveness and superiority of the proposed load-sharing-based improved FMEA method, a comparative analysis was conducted against two classical approaches: the Traditional FMEA method, which ranks failure modes by directly multiplying the expert-rated S, O, and D values to obtain the RPN; and the PLTS-FBWM-TOPSIS method without load sharing, which employs the same PLTS for processing expert assessments, the FBWM for calculating weights, and TOPSIS for ranking, but does not incorporate any system data derived from load sharing. The comparative results are detailed in Table 11.

Table 11. Ranking results under different methods.

	FMEA		**PLTS-FBWM-TOPSIS**		**This Method**	
	Score	**RANK**	**C_i**	**RANK**	**C_i**	**RANK**
FM1	56.15464	10	0.417681	3	0.395978	3
FM2	81.03893	3	0.688908	1	0.709816	1
FM3	59.51582	9	0.368913	6	0.366015	6
FM4	70.99446	4	0.373307	5	0.35748	7
FM5	65.76415	8	0.330949	8	0.335865	8
FM6	97.21092	2	0.628241	2	0.655803	2
FM7	65.9413	7	0.35927	7	0.370895	5
FM8	120.7705	1	0.409778	4	0.384757	4
FM9	66.99181	5	0.216856	12	0.181522	12
FM10	42.41067	11	0.299069	9	0.284656	9
FM11	40.6663	12	0.256036	10	0.26432	11
FM12	66.54952	6	0.237386	11	0.268983	10

As can be seen from the above table, in the traditional FMEA method, FM8 ranks first and FM6 ranks second. Both FM6 and FM8 belong to the magnetic system. This ranking occurs because the traditional FMEA does not consider the weights of RFs. In the method without considering load sharing data, FM2 ranks first. Moreover, the rankings of FM4 and FM7 are quite different from those of the method proposed in this paper. This is because, when spatial factors are taken into account, FM4 is surrounded by more components, so its ranking rises, while FM7 has fewer surrounding components, leading to a decline in its ranking.

To verify the advantages of this method over other methods, we adjust the weights of S, O, and D: gradually reduce the weight of S by 0.01 and gradually increase the weight of O by 0.01, dividing into nine groups in total. We then calculate the standard deviation of C_i for the nine groups. For the traditional FMEA method, we set the initial weights to be equal, and the specific details are shown in Table 12.

As shown in Figure 6, the analysis reveals that the standard deviations for all failure modes under the traditional FMEA method are substantially higher than those of the other two methods. This indicates that the traditional method is highly sensitive to the setting of risk factor weights; minor changes can lead to significant fluctuations in the ranking results, which is a major drawback in practical applications. In contrast, the PLTS-FBWM-TOPSIS method shows a marked reduction in standard deviation, demonstrating the enhanced stability offered by MCDM methods. Crucially, the proposed method achieves the smallest standard deviation for the majority of failure modes (e.g., FM1, FM4, FM9, FM10, FM11, and FM12). This provides strong evidence that the objective system structural

information introduced by load sharing effectively counteracts the uncertainty inherent in subjective weight assignments, thereby endowing the overall risk assessment model with superior robustness.

Table 12. Comparison of different methods.

	FMEA	PLTS-FBWM-TOPSIS	This Method
	S.D.	S.D.	S.D.
FM1	0.061956	0.006072	0.002804
FM2	0.089411	0.02695	0.029429
FM3	0.065664	0.011418	0.009803
FM4	0.078329	0.00605	0.0005
FM5	0.072558	0.00755	0.015694
FM6	0.107253	0.02727	0.030127
FM7	0.072753	0.011893	0.019782
FM8	0.133247	0.002238	0.004481
FM9	0.073912	0.013117	0.012297
FM10	0.046792	0.028929	0.009267
FM11	0.044867	0.026442	0.003473
FM12	0.073424	0.020027	0.011247

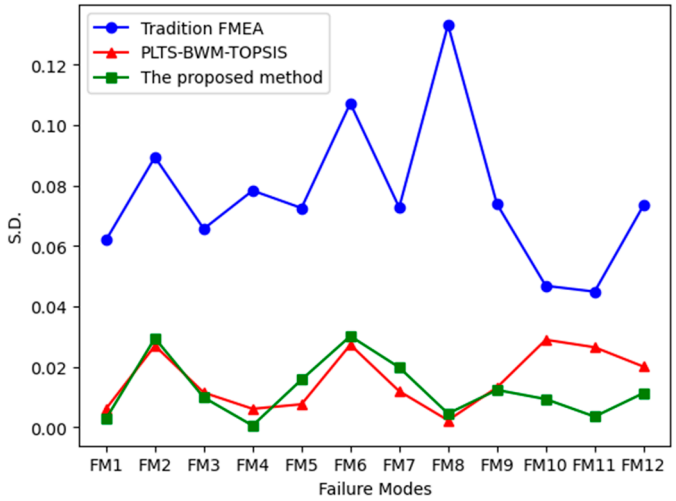


Figure 6. Standard deviation of failure modes under different methods.

5. Conclusions

This study addresses the limitations of traditional FMEA, such as neglecting inherent systemic structural information, equalizing RF weights, and a strong subjectivity in risk ranking, by proposing an improved FMEA method integrated with the load sharing principle. The method quantifies experts' assessments using PLTS and aggregates multiple expert opinions via the geometric mean, determines the relative weights of S, O, and D with the FBWM, derives objective system failure probability data through load sharing modeling based on component spatial connections, and finally integrates subjective–objective data and weights into TOPSIS for comprehensive risk ranking. Validated on a multi-magnetic system magnetic crane, comparative experiments with traditional FMEA and PLTS-FBWM-TOPSIS confirm that the proposed method exhibits superior accuracy, stability, and objectivity in risk prioritization, providing reliable support for the risk assessment of complex multi-component systems.

In the future work, we want to integrate finite element analysis or multi-body dynamics simulation into expert evaluations to reduce the subjectivity in S, O, and D assessment,

as well as expand the method's application to load sharing systems like gearboxes and turbine rotors.

Author Contributions: B.S.: Writing—review and editing, Writing—original draft, Validation, Supervision, Resources, Project administration, Funding acquisition, Formal analysis, and Conceptualization. L.W.: Writing—original draft, Visualization, Validation, Software, Methodology, Investigation, Formal analysis, and Data curation. J.Z.: Supervision, Resources, Investigation, and Formal analysis. N.D.: Resources and Investigation. All authors have read and agreed to the published version of the manuscript.

Funding: This research was funded by the Jilin Provincial Science and Technology Development Plan, grant number YDZJ202401303ZYTS.

Data Availability Statement: Data will be made available on request.

Conflicts of Interest: The authors declare no conflicts of interest.

Appendix A

In Section 3.3, the expert-provided Occurrence (O) ratings are first quantified and aggregated. This aggregated value is then converted into its corresponding probabilistic form, denoted as $E = \{e_1, e_2, \ldots, e_n\}$.

Appendix A.1. Derivation When Components Are Mutually Independent

Define the Failure Probability of the Next State:

The probability of transitioning from the initial state to the next failure mode is given by the set S. If no failure occurs, it is expressed as shown in Formula (A1).

$$e_{\mathrm{i}} = e_j \tag{A1}$$

Assume that when component j around component i fails, the load on component i will increase, and thus its probability of failure will rise, as expressed in Formula (A2).

$$e_{i(j)} = (1 + \frac{z_{i(j)}}{L})e_i \tag{A2}$$

Assume that when component j fails, if the nearby components fail, the formula is as shown in Formula (A3).

$$e_{i(\mathrm{j,k})} = (1 + \frac{z_{i(\mathrm{j,k})}}{L})e_i \tag{A3}$$

Under the condition of component independence, the final derived method is as follows:

$$F_{i(j_1,j_2,j_3,\ldots,j_n)} = e_{j_1} \times e_{j_2(j_1)} \times e_{j_3(j_1,j_2)} \times \cdots \times e_{j_n(j_1,j_2,\ldots,j_{n-1})} \times e_{i(j_1,j_2,\ldots j_n)} \tag{A4}$$

Appendix A.2. Derivation When Components Are Interrelated

In the single scenario described in Appendix A.1, the situation occurs only when the failed components $j_1, j_2, j_3, \ldots, j_n$ are mutually independent. If there are m interrelated components among $j_1, j_2, j_3, \ldots, j_n$, different sequences of components may result in $m!$ outcomes for F. In this section, we will address this issue by aggregating multiple outcomes into a single result.

Define the sequences of independent and interrelated components:

When there are n components around component i, there are $n!$ possible sequences, as shown in Formula (A5). If these n components are mutually independent, changes in their sequence will have no impact, as shown in Formula (A6).

$$\left\{F_{i(j_1,j_2,j_3,\ldots,j_n)}, F_{i(j_2,j_1,j_3,\ldots,j_n)}, F_{i(j_3,j_2,j_1,\ldots,j_n)}, \ldots, F_{i(j_n,j_{n-1},j_{n-2},\ldots,j_1)}\right\} \tag{A5}$$

$$F_{i(j_1,j_2,j_3,\ldots,j_n)} = F_{i(j_2,j_1,j_3,\ldots,j_n)} = F_{i(j_3,j_2,j_1,\ldots,j_n)} = \ldots = F_{i(j_n,j_{n-1},j_{n-2},\ldots,j_1)} \tag{A6}$$

If, among these n components, m are interrelated with each other, there can be at most $m!$ distinct outcomes for O. Since independent components have no impact on the result regardless of their positions, we divide O into two subsets: set A, consisting of interrelated components, and set B, consisting of mutually independent components, as shown in Formula (A7).

$$\begin{cases} A = \{a_1, a_2, \ldots, a_m\} \\ B = \{b_1, b_2, \ldots, b_s\} \end{cases}, m + s = n, F = \{A, B\} \tag{A7}$$

Calculation of Independent Components:

Since the order of components in set B does not affect the result, we will only consider the order of components in set A as shown in Set (A8). Therefore, we derive the result for set B as shown in Formula (A9).

$$\left\{F_{i(a_1,a_2,a_3,\ldots,a_m)}, F_{i(a_2,a_1,a_3,\ldots,a_m)}, F_{i(a_3,a_2,a_1,\ldots,a_m)}, \ldots, F_{i(a_m,a_{m-1},a_{m-2},\ldots,a_1)}\right\} \tag{A8}$$

$$F_B = e_{b_1} \times e_{b_2} \times \cdots \times e_{b_s} \tag{A9}$$

Calculation of All Sequential Values of F:

There are $m!$ possible sequences for set A, as shown in Set (A10), and all corresponding results are presented in Formula (A11).

$$F_s = \left\{F_{i(a_1,a_2,a_3,\ldots,a_m)}, F_{i(a_2,a_1,a_3,\ldots,a_m)}, F_{i(a_3,a_2,a_1,\ldots,a_m)}, \ldots, F_{i(a_m,a_{m-1},a_{m-2},\ldots,a_1)}\right\} \tag{A10}$$

$$\begin{cases} F_{i(a_1,a_2,a_3,\ldots,a_m)} = e_{a_1} \times e_{a_2(a_1)} \times \cdots \times e_{a_n(a_1,a_2,\ldots,a_{m-1})} \times e_{i(a_1,a_2,\ldots a_m)} \times F_B \\ F_{i(a_2,a_1,a_3,\ldots,a_m)} = e_{a_2} \times e_{a_1(a_2)} \times \cdots \times e_{a_n(a_2,a_1,\ldots,a_{m-1})} \times e_{i(a_2,a_1,\ldots a_m)} \times F_B \\ F_{i(a_3,a_2,a_1,\ldots,a_m)} = e_{a_3} \times e_{a_2(a_3)} \times \cdots \times e_{a_n(a_3,a_2,\ldots,a_{m-1})} \times e_{i(a_3,a_2,\ldots a_m)} \times F_B \\ \vdots \\ F_{i(a_n,a_{n-1},a_{n-2},\ldots,a_1)} = e_{a_m} \times e_{a_{m-1}(a_m)} \times \cdots \times e_{a_1(a_m,a_{m-1},\ldots,a_2)} \times e_{i(a_m,a_{m-1},\ldots a_1)} \times F_B \end{cases} \tag{A11}$$

Weight Calculation and Aggregation of All Different Sequences:

If there are m interrelated components among the n components, the results for all different sequences of the interrelated components are calculated using Formula (A4), as shown in Formula (A12). A larger value indicates a higher occurrence probability and thus a greater weight, with the weight calculation formula presented in Formula (A13).

$$\begin{cases} D_1 = F_{(a_1,a_2,a_3,\ldots,a_m)} = e_{a_1} \times e_{a_2(a_1)} \times e_{a_3(a_1,a_2)} \times \cdots \times e_{a_n(a_1,a_2,\ldots,a_{m-1})} \\ D_2 = F_{(a_2,a_1,a_3,\ldots,a_m)} = e_{a_2} \times e_{a_1(a_2)} \times e_{a_3(a_2,a_1)} \times \cdots \times e_{a_n(a_2,a_1,\ldots,a_{m-1})} \\ D_3 = F_{(a_3,a_2,a_1,\ldots,a_m)} = e_{a_3} \times e_{a_2(a_3)} \times e_{a_1(a_3,a_2)} \times \cdots \times e_{a_n(a_3,a_2,\ldots,a_{m-1})} \\ \vdots \\ D_{m!} = F_{(a_n,a_{n-1},a_{n-2},\ldots,a_1)} = e_{a_m} \times e_{a_{m-1}(a_m)} \times e_{a_{m-2}(a_m,a_{m-1})} \times \cdots \times e_{a_1(a_m,a_{m-1},\ldots,a_2)} \end{cases} \tag{A12}$$

$$w_i = \frac{D_i}{\sum_{i=1}^{m!} D_i} \tag{A13}$$

By weighted averaging w_i into the set F_s, the final aggregated result is obtained as shown in Formula (A14).

$$F_i = w_1 \times F_{i(a_1,a_2,a_3,\ldots,a_m)} + w_2 \times F_{i(a_2,a_1,a_3,\ldots,a_m)} + \ldots, + w_{m!} \times F_{i(a_m,a_{m-1},a_{m-2},\ldots,a_1)} \quad \text{(A14)}$$

To illustrate how to calculate the occurrence probability of a failure mode, we use Figure A1 for description. Components B, C, and D are unconnected with no interrelationships, and they do not bear each other's loads when failing. Only after B, C, and D fail simultaneously will the failure of Component A lead to system failure. B, C, and D are mutually independent, so their individual failures do not affect each other's failure probabilities. After B, C, and D fail, Component A will bear the loads originally assigned to B, C, and D, resulting in increased load and a higher probability of failure. This is related to the proportion of loads that B, C, and D distribute to A. Calculating the data for A means determining the conditions under which A's failure will cause system failure.

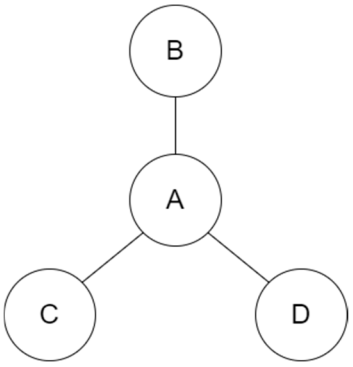


Figure A1. An unrelated Four-component system.

Calculate the occurrence probability $F_{\mathrm{A}} = e_{\mathrm{B}} \times e_C \times e_D \times e_{A(B,C,D)}$ of Component A, where $e_{\mathrm{B}} = e^*_{\mathrm{B}}$, $e_{\mathrm{C}} = e^*_{\mathrm{C}}$, $e_{\mathrm{D}} = e^*_{\mathrm{D}}$, $e_{A(B,C,D)} = (1 + \frac{z_{A(B,C,D)}}{L})e_A$.

The above calculation is based on the scenario where the surrounding components of the target component have no interrelationships and the failure sequence does not affect the final result. However, if the surrounding components are interrelated, different failure sequences will lead to different final results, as shown in Figure A2. When analyzing Component A, the failure sequence of Component B does not affect the final result, but the failures of Components C and D will affect their own loads, resulting in an increased probability of failure.

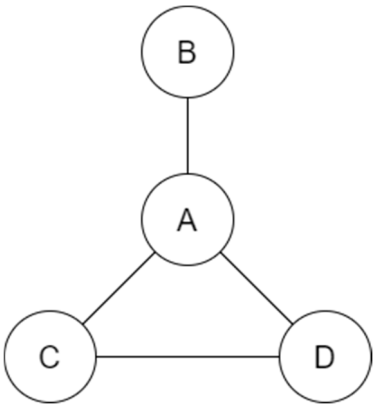


Figure A2. A related Four-component system.

When Component C fails first and Component D subsequently fails, $F_{A(C,D)} = e_B \times e_C \times e_{D(C)} \times e_{A(B,C,D)}$. When Component D fails first and Component C subsequently fails, $F_{A(D,C)} = e_B \times e_D \times e_{C(D)} \times e_{A(B,C,D)}$.

To integrate these two scenarios, the one with a higher occurrence probability is assigned a greater weight. The weights of Components C and D are calculated as shown in Formula (A15).

$$\begin{cases} w_C = \frac{e_C \times e_{D(C)}}{e_C \times e_{D(C)} + e_D \times e_{C(D)}} \\ w_D = \frac{e_D \times e_{C(D)}}{e_C \times e_{D(C)} + e_D \times e_{C(D)}} \end{cases} \tag{A15}$$

The final simplified result is $F_A = w_C F_{A(C,D)} + w_D F_{A(D,C)}$.

References

1. Wang, L.; Li, B.; Hu, B.; Shen, G.; Zheng, Y.; Zheng, Y. Failure mode effect and criticality analysis of ultrasound device by classification tracking. *BMC Health Serv. Res.* **2022**, *22*, 429. [CrossRef]
2. Wu, Z.; Liu, W.; Nie, W. Literature review and prospect of the development and application of FMEA in manufacturing industry. *Int. J. Adv. Manuf. Technol.* **2021**, *112*, 1409–1436. [CrossRef]
3. Naranjo, J.E.; Alban, J.S.; Balseca, M.S.; Bustamante Villagómez, D.F.; Mancheno Falconi, M.G.; Garcia, M.V.J.S. Enhancing Institutional Sustainability Through Process Optimization: A Hybrid Approach Using FMEA and Machine Learning. *Int. J. Adv. Manuf. Technol.* **2025**, *17*, 1357. [CrossRef]
4. Shi, H.; Wang, L.; Li, X.-Y.; Liu, H.-C. A novel method for failure mode and effects analysis using fuzzy evidential reasoning and fuzzy Petri nets. *J. Ambient Intell. Humaniz. Comput.* **2020**, *11*, 2381–2395. [CrossRef]
5. Tian, Y.; Song, S.; Zhou, D.; Pang, S.; Wei, C. Canonical triangular interval type-2 fuzzy set linguistic distribution assessment TODIM approach: A case study of FMEA for electric vehicles DC charging piles. *Expert Syst. Appl.* **2023**, *223*, 119826. [CrossRef]
6. Li, A. Risk assessment of crane operation hazards using modified FMEA approach with Z-Number and set pair analysis. *Heliyon* **2024**, *10*, e28603. [CrossRef]
7. Pang, Q.; Wang, H.; Xu, Z. Probabilistic linguistic term sets in multi-attribute group decision making. *Inf. Sci.* **2016**, *369*, 128–143. [CrossRef]
8. Farhadinia, B.; Liao, H. Group decision making based on the relationships between the information measures for additive and multiplicative linguistic term sets. *Soft Comput.* **2019**, *23*, 7901–7911. [CrossRef]
9. Ma, X.; Han, X.; Xu, Z.; Rodriguez, R.M.; Zhan, J. Fusion of probabilistic linguistic term sets for enhanced group decision-making: Foundations, survey and challenges. *Inf. Fusion* **2025**, *116*, 102802. [CrossRef]
10. Gou, X.; Xu, Z.; Liao, H.; Herrera, F. Probabilistic double hierarchy linguistic term set and its use in designing an improved VIKOR method: The application in smart healthcare. *J. Oper. Res. Soc.* **2021**, *72*, 2611–2630. [CrossRef]
11. Wang, Z.-C.; Ran, Y.; Chen, Y.; Yang, X.; Zhang, G. Group risk assessment in failure mode and effects analysis using a hybrid probabilistic hesitant fuzzy linguistic MCDM method. *Expert Syst. Appl.* **2022**, *188*, 116013. [CrossRef]
12. Lo, H.-W.; Shiue, W.; Liou, J.J.; Tzeng, G.-H. A hybrid MCDM-based FMEA model for identification of critical failure modes in manufacturing. *Soft Comput.* **2020**, *24*, 15733–15745. [CrossRef]
13. Kumari, S.; Ahmad, K.; Khan, Z.A.; Ahmad, S. Analysing the failure modes of water treatment plant using FMEA based on fuzzy AHP and fuzzy VIKOR methods. *Arab. J. Sci. Eng.* **2025**, *50*, 16821–16836. [CrossRef]
14. Li, H.; Díaz, H.; Soares, C. A failure analysis of floating offshore wind turbines using AHP-FMEA methodology. *Ocean Eng.* **2021**, *234*, 109261. [CrossRef]
15. Rezaei, J. Best-worst multi-criteria decision-making method. *Omega* **2015**, *53*, 49–57. [CrossRef]
16. Pamučar, D.; Ecer, F.; Cirovic, G.; Arlasheedi, M. Application of improved best worst method (BWM) in real-world problems. *Mathematics* **2020**, *8*, 1342. [CrossRef]
17. Liou, J.J.; Guo, B.H.; Huang, S.-W.; Yang, Y.-T. Failure mode and effect analysis using interval type-2 fuzzy and multiple-criteria decision-making methods. *Mathematics* **2024**, *12*, 3931. [CrossRef]
18. Xue, Y.; Zhang, J.; Zhang, Y.; Yu, X. Barrier assessment of EV business model innovation in China: An MCDM-based FMEA. *Transp. Environ.* **2024**, *136*, 104404. [CrossRef]
19. Kuchekar, P.; Bhongade, A.S.; Rehman, A.U.; Mian, S.H. Assessing the Critical Factors Leading to the Failure of the Industrial Pressure Relief Valve Through a Hybrid MCDM-FMEA Approach. *Machines* **2024**, *12*, 820. [CrossRef]
20. Shafizadeh, E.; Hossein Mousavizadegan, S. A comprehensive risk assessment framework for composite Lenj Hulls: Integrating FMEA with CRITIC-CODAS. *Civ. Eng. Environ. Syst.* **2025**, 1–21. [CrossRef]

21. Wang, J.; Zhang, J.; Wu, J.; Zhang, Q.; Fang, Y.; Huang, X. Optimal inspection-based maintenance strategy for k-out-of-n: G load-sharing systems consisting of three-state components. *Comput. Ind. Eng.* **2025**, *209*, 111446. [CrossRef]
22. Singh, B.; Gupta, P.K. Load-sharing system model and its application to the real data set. *Math. Comput. Simul.* **2012**, *82*, 1615–1629. [CrossRef]
23. Seikh, M.R.; Chatterjee, P. Sustainable strategies for electric vehicle adoption: A confidence level-based interval-valued spherical fuzzy MEREC-VIKOR approach. *Inf. Sci.* **2025**, *699*, 121814. [CrossRef]
24. Al-Abadi, A.M.; Handhal, A.M.; Abdulhasan, M.A.; Ali, W.L.; Hassan, J.; Al Aboodi, A.H. Optimal siting of large photovoltaic solar farms at Basrah governorate, Southern Iraq using hybrid GIS-based Entropy-TOPSIS and AHP-TOPSIS models. *Renew. Energy* **2025**, *241*, 122308. [CrossRef]
25. Behzadian, M.; Otaghsara, S.K.; Yazdani, M.; Ignatius, J. A state-of the-art survey of TOPSIS applications. *Expert Syst. Appl.* **2012**, *39*, 13051–13069. [CrossRef]
26. Zhao, S.; Wei, Y.; Li, Y.; Cheng, Y. A multi-agent reinforcement learning (MARL) framework for designing an optimal state-specific hybrid maintenance policy for a series *k*-out-of-*n* load-sharing system. *Reliab. Eng. Syst. Saf.* **2025**, *265*, 111587. [CrossRef]
27. Krejčí, J.; Stoklasa, J. Aggregation in the analytic hierarchy process: Why weighted geometric mean should be used instead of weighted arithmetic mean. *Expert Syst. Appl.* **2018**, *114*, 97–106. [CrossRef]
28. Bahrami, S.; Rastegar, M.; Dehghanian, P. An fbwm-topsis approach to identify critical feeders for reliability centered maintenance in power distribution systems. *Manuf. Rev.* **2020**, *15*, 3893–3901. [CrossRef]
29. Xiao, Z.; Shi, Z.; Bai, J. FMEA Risk Assessment Method for Aircraft Power Supply System Based on Probabilistic Language-TOPSIS. *Aerospace* **2025**, *12*, 548. [CrossRef]
30. Trung, D.D. Development of data normalization methods for multi-criteria decision making: Applying for MARCOS method. *Manuf. Rev.* **2022**, *9*, 22. [CrossRef]
31. Zhou, X.; Tang, Y. Modeling and fusing the uncertainty of FMEA experts using an entropy-like measure with an application in fault evaluation of aircraft turbine rotor blades. *Entropy* **2018**, *20*, 864. [CrossRef] [PubMed]
32. Zhuo, Y.; Ma, L.; Li, C.; Chen, X. Risk analysis and mitigation of pressurization test for civil aircraft airtight cabin doors based on FMEA. *J. Phys. Conf. Ser.* **2025**, *3080*, 012142. [CrossRef]

Disclaimer/Publisher's Note: The statements, opinions and data contained in all publications are solely those of the individual author(s) and contributor(s) and not of MDPI and/or the editor(s). MDPI and/or the editor(s) disclaim responsibility for any injury to people or property resulting from any ideas, methods, instructions or products referred to in the content.